2-26-2003

Anchoring-Mediated Interaction of Edge Dislocations With Bounding Surfaces in Confined Cholesteric Liquid Crystals

Ivan I. Smalyukh
Kent State University - Kent Campus

Oleg Lavrentovich
Kent State University - Kent Campus, olavrent@kent.edu

Anchoring-Mediated Interaction of Edge Dislocations with Bounding Surfaces in Confined Cholesteric Liquid Crystals

I. I. Smalyukh and O. D. Lavrentovich*

Chemical Physics Interdisciplinary Program and Liquid Crystal Institute, Kent State University, Kent, Ohio 44242

(Received 3 September 2002; published 26 February 2003)

We employ the fluorescent confocal polarizing microscopy to image edge dislocations in cholesteric liquid crystals. Surface anchoring at the bounding plates determines the structure and behavior of defects. Two types of plates set in-plane director orientation but differ in the type of associated anchoring potentials. Plates with strong polar anchoring and nonzero azimuthal anchoring repel the dislocations, while plates with weak polar anchoring and no azimuthal anchoring allow the dislocations to escape through the boundary. To explain the results, we propose a coarse-grained model of cholesteric anchoring.

DOI: 10.1103/PhysRevLett.90.085503 PACS numbers: 61.30.Hn, 61.30.Eb, 61.72.Lk, 87.64.Tt

Interaction between a dislocation and a bounding surface is an important problem in soft matter physics [1,2]. For lamellar phases such as diblock copolymers, smectic and cholesteric liquid crystals (CLCs), theoretical models predict that an edge dislocation is either attracted to or repelled from the surface, depending on the surface-tension and elastic constants of the material [1]. There are no direct experiments to confirm the theory, as imaging of dislocations is difficult. Transmission electron microscopy allowed Maaloum *et al.* [3] to visualize a dislocation beneath the free surface of diblock copolymers but not its possible glide. Furthermore, the available models consider only the surface-tension contribution to the surface energy, and neglect the anchoring part, associated with a variation of layers tilt at the boundary.

At large scales, a CLC is described as a lamellar phase [4]. In CLC, the director $\mathbf{n} = -\mathbf{n}$ is helicoidally twisted with a pitch p; the period $p/2$ is a thickness of an elementary CLC ''lamella.'' Defects in CLC can be studied by optical means when $p \gtrsim 1$ μm. We employ the new nondestructive technique of fluorescent confocal polarizing microscopy (FCPM) [5–7] to image edge dislocations and their glide in CLC. We demonstrate that the edge dislocation glides towards or away from the boundary, depending on the surface anchoring. The surface-tension effect is excluded as the CLC is confined between rigid plates. We propose a coarse-grained model of CLC anchoring to explain the observed phenomena.

FCPM has two distinctive features [5,6]: (i) excitation light is linearly polarized and (ii) the CLC is doped with fluorescent dye molecules aligned by $\mathbf{n}$. The intensity of the detected fluorescent signal is a function of the angle β between the transition dipole of dye molecules (parallel to $\mathbf{n}$) and polarization $\mathbf{P}$ of testing light, $I \propto \cos^4\beta$ [5,6]. The focused beam scans the sample in the horizontal plane, at any prefixed depth z. Scanning at different depths results in a 3D director image with a ~ 1 μm resolution. The vertical slices reveal the CLC structure across the sample; it appears as a pattern of bright ($\mathbf{n} \parallel \mathbf{P}$) and dark ($\mathbf{n} \perp \mathbf{P}$) stripes. The CLC was formed by the nematic material ZLI3412 (EM Industries) doped with a chiral agent CB15 (EM Industries, $\sim 3.2\%$ by weight, $p = 5$ μm), and with a tiny amount ~ 0.01 wt% of dye n,n'-bis(2,5-di-tert-butylphenyl)-3,4,9,10-perylenedicarboximide (BTBP, Molecular Probes) [5–7]. Low birefringence of ZLI3412, $\Delta n \approx 0.07$, helps to mitigate defocusing effects [5] and to avoid the Mauguin regime [6].

We use flat cells and wedge cells with a small dihedron angle $\alpha = 0.45°$, confined between glass plates of thickness 0.15 mm. There are two types of polymer aligning layers, denoted SU and WD. Both align $\mathbf{n}$ in the plane of the plate (pretilt angle $\lesssim 1°$) but with very different anchoring energies. The first symbol refers to the polar anchoring coefficient W_p (S for ''strong'' and W for ''weak'') that characterizes the work needed to deviate $\mathbf{n}$ in the plane perpendicular to the substrate; W_p for ZLI3412 is measured by retardation vs the voltage method [8]. The second symbol refers to the azimuthal (''in-plane'') anchoring which was either degenerate (D) or uniaxial (U). The SU plates are coated with unidirectionally buffed PI2555 (HD MicroSystems) with large $W_p = (4 \pm 1) \times 10^{-4}$ J/m^2 and small $W_a \sim 10^{-5}$ J/m^2 [7]. The WD plates use nonrubbed polyisoprene with relatively small $W_p = (0.7 \pm 0.6) \times 10^{-4}$ J/m^2 and $W_a = 0$; even if there is any residual in-plane anchoring, W_a is smaller than 3×10^{-10} J/m^2 [9].

The equilibrium state of wedge samples with two SU plates is a lattice of edge dislocations [7]. The Burgers vector is $b = p/2$ for dislocations in the thin part and $b = p$ above some critical thickness. The core of a $b = p$ dislocation splits into a pair of disclinations with nonsingular core ($\mathbf{n}$ is along the defect axis) [7]. These disclinations are $\lambda^{+1/2}$ and $\lambda^{-1/2}$ lines in Kleman-Friedel classification [2]. Each $b = p$ dislocation separates two neighboring domains (Grandjean zones) of the wedge in which the number N of cholesteric layers (each of thickness $p/2$) changes by $\Delta N = 2$. Dislocations tend to accumulate in the bisector plane of the wedge,

although their glide is hindered by Peierls-Nabarro friction [7].

FCPM of well-equilibrated CLC wedges with one WD plate and one SU plate reveals no bulk dislocations, in accordance with the regular microscopy observations [10]. As thickness of the wedge changes, the number of CLC layers changes by an insertion/removal of a layer near the WD plate rather than by bulk dislocations (Fig. 1). The edge dislocations can be found as transient features of a filling process or after a rapid temperature quench from the isotropic phase. Their Burgers vector is always $b = p$; the core is a $\lambda^{-1/2}\lambda^{+1/2}$ pair (Fig. 2). Despite the fact that each $b = p$ dislocation introduces $\Delta N = 2$, the neighboring Grandjean zones differ only by $\Delta N = 1$. The fit is achieved by a removal of one layer at the WD boundary (Fig. 2). The dislocations slowly glide towards the WD plate [Figs. 2(a)–2(c)] and coalesce with the surface layer [Fig. 2(d)]. Dislocations do not glide as straight lines but via kinks, similarly to the situation in SU samples [7].

In flat cells with both substrates of WD type, the transient dislocations are accompanied by two surface layers (Fig. 3). Importantly, the dislocation profile in this sample is well fitted by the nonlinear Brener-Marchenko elastic theory of an isolated edge dislocation in an *infinite* medium [11,12] [Fig. 3(b)]. The physical implication is that the interaction between the dislocation and the surfaces is close to zero (neither attraction nor repulsion).

In the phenomena described above, the surface tension is irrelevant, and the dislocation-rigid plate interaction is controlled by the anisotropic (anchoring) part of surface energy. As seen in Figs. 1–3, CLC layers are tilted at WD plates; near the SU plates, the surface layers run parallel to the boundaries [7]. When $W_p = W_a = 0$, the dislocation is attracted to the plate and escapes from the CLC slab, as the net result is the decrease of elastic energy. When $W_p \to \infty$, $W_a \to \infty$, the dislocation is pushed into CLC bulk, as the layers should be parallel to the flat plates. For the SU-SU wedge, the equilibrium location of dislocation is in the bisector plane [7]. To cast some light on intermediate situations, we present a coarse-grained model of CLC anchoring, valid for a D plate with $0 < W_p < \infty$ and $W_a = 0$; as we shall see, the model allows one to understand both WD and SU samples.

A semi-infinite CLC is bounded by a plate at $z = 0$ that sets the helicoid axis $\mathbf{t}$ parallel to the normal $\boldsymbol{\nu}$ to plate. An external torque sets a nonzero angle $0 \le \theta_\infty \le \pi/2$ between $\mathbf{t}$ and $\boldsymbol{\nu}$ far away from the boundary at $z \to \infty$. The dependence $\theta(z)$ is determined by the anchoring potential experienced by $\mathbf{t}$ at the surface and by the elastic energy of bulk distortions (Fig. 4). The elastic energy density [2],

$$f = \frac{1}{2}K_1(\mathrm{div}\mathbf{t})^2 + \frac{1}{2}K_3(\mathbf{t}\times\mathrm{curl}\mathbf{t})^2 + \frac{1}{2}B\left(\frac{p-p_0}{p_0}\right)^2, \quad (1)$$

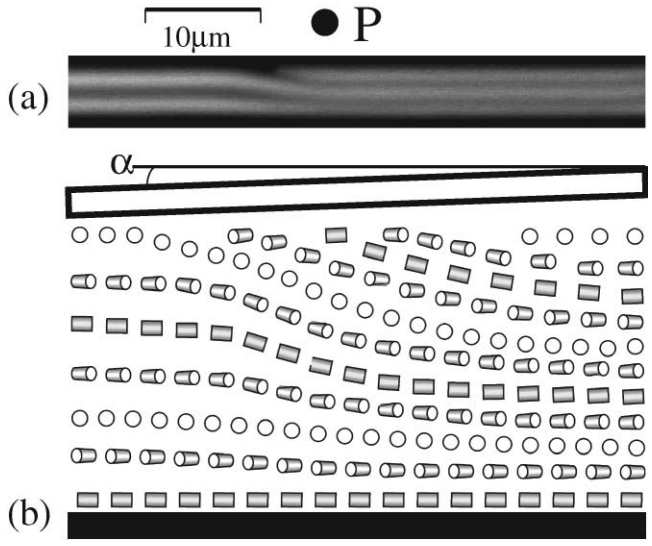

FIG. 1. FCPM vertical cross sections (a) and director field (b) of the thin part of a cholesteric wedge cell (local thickness $\sim 5\ \mu$m) with top WD plate and bottom SU plate.

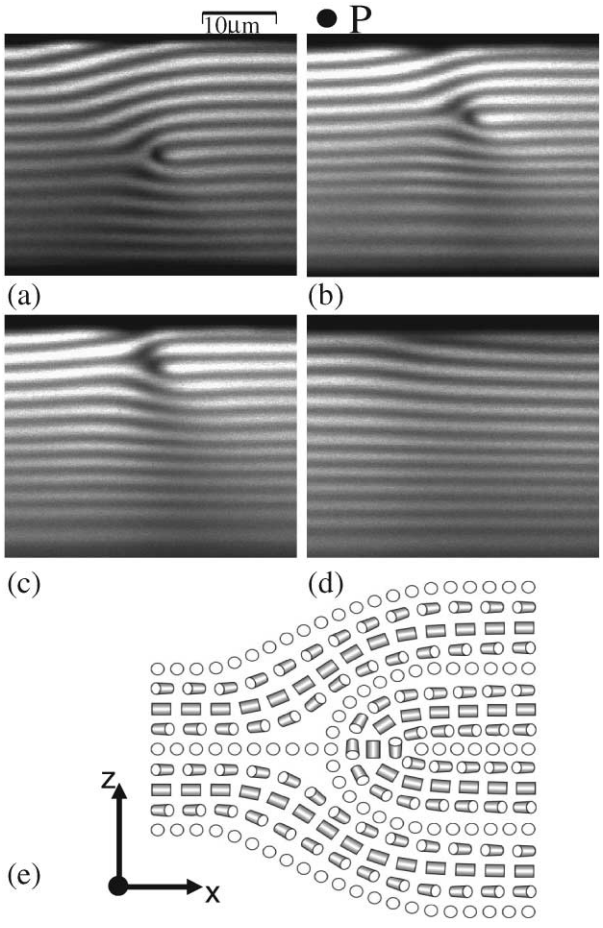

FIG. 2. FCPM textures (a)–(d) of a dislocation gliding towards the WD plate and away from the SU plate; local thickness $\sim 30\ \mu$m; (e) director field near the dislocation core.

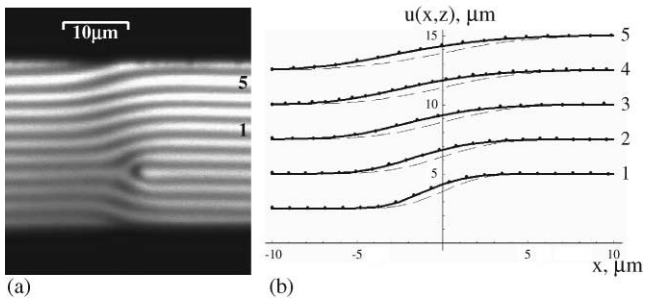

FIG. 3. A dislocation in a flat cell of thickness $\sim 30\ \mu$m bounded by two WD plates (a); nonlinear theory for an infinite medium (lines) fits the experimental profile (dots) well while the linear theory (dashed lines) does not. Fitting parameters: $K_1 = 3K_{33}/8 = 5.8$ pN; $B = K_{22}(2\pi/p)^2 = 10.6$ J/m^3; $p = 5\ \mu$m.

includes splay, bend, and dilation terms with the moduli K_1, K_3, and B, respectively; p and p_0 are the actual and the equilibrium values of the cholesteric pitch. With $\mathbf{t} = (\sin\theta, 0, \cos\theta)$, the free energy per unit area of the boundary is

$$W_t = \frac{1}{2}\int_0^\infty \left[K_3 \cos^2\theta \left(\frac{\partial\theta}{\partial z}\right)^2 + B\left(\frac{\sin\theta}{\sin\theta_\infty} - 1\right)^2 \right] dz + \frac{1}{4} W_p \sin^2\theta|_{z=0}. \quad (2)$$

The last term is calculated as follows. Director deviations from the equilibrium orientation $\mathbf{n} \perp \boldsymbol{\nu}$ are described by the Rapini-Papoular anchoring potential: $W_n = W_p(\mathbf{n}\cdot\boldsymbol{\nu})^2/2$. For CLC, W_n has to be averaged over director rotations, which yields $\langle W_n\rangle = \frac{1}{4} W_p \sin^2\theta|_{z=0}$. In the elastic part of W_t, the term $K_1 \sin^2\theta(\frac{\partial\theta}{\partial z})^2$ is neglected, as we assume $\theta \ll 1$. Minimization of W_t yields the layers profile $t_x(z) = \sin\theta(z)$ near the boundary, and the coarse-grained anchoring potential W_t for $\mathbf{t}$:

$$t_x(z) = \sin\theta_\infty \left[1 - \frac{W_p \sin\theta_\infty}{2B\lambda_3 + W_p \sin\theta_\infty} \exp\left(-\frac{z}{\lambda_3 \sin\theta_\infty}\right)\right], \quad (3)$$

$$W_t(\theta_\infty) = \frac{W_p B \lambda_3 \sin^2\theta_\infty}{4B\lambda_3 + 2W_p \sin\theta_\infty}, \quad (4)$$

where $\lambda_3 = \sqrt{K_3/B}$. The distortions decay exponentially within a subsurface slab of a small thickness $\lambda_3 \sin\theta_\infty$; outside it, $\theta \approx \theta_\infty$ (Fig. 4(b)).

Let us now estimate the changes in the elastic and anchoring energies as an edge dislocation is transferred from the depth $z = d''$ to $d' < d''$ in a semi-infinite sample; d' is larger than the typical core size of the dislocation $\sim p$; the coarse-grained model is not applicable when $d \lesssim p$. The equilibrium configuration of layers around a dislocation in an infinite sample is [1,2] $u(x,z) = \frac{b}{4}\{1 + \mathrm{erf}[x/2\sqrt{\lambda_1(z-d)}]\}$, where $\lambda_1 = \sqrt{K_1/B}$; the result corresponds to the linear elastic model [2].

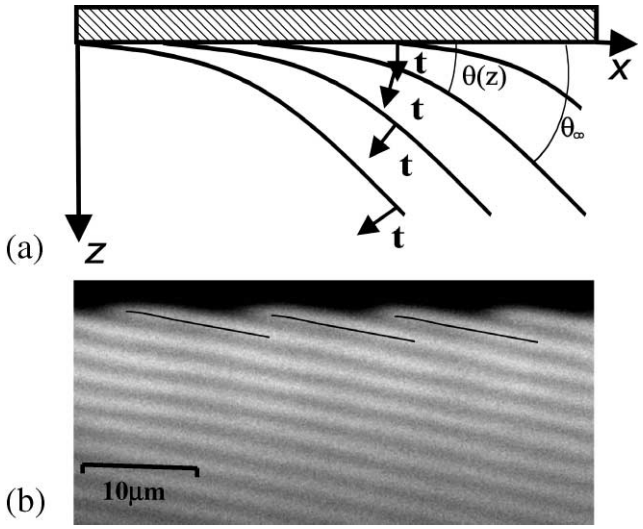

FIG. 4. The scheme (a) and the FCPM texture (b) of CLC layers near a WD plate illustrating spatial relaxation of the tilted layers; the solid lines are calculated from Eq. (3). The tilt of the layers was induced by a magnetic field making the angle θ_∞ with the plate; the texture was recorded immediately after the field was switched off.

Integrating the elastic energy density $f_{\mathrm{el}} = K_1(\frac{\partial^2 u}{\partial x^2})^2 + B(\frac{\partial u}{\partial z})^2$ over $-\infty < x < \infty$; $0 < z < d''$ and subtracting a similar quantity integrated over $0 < z < d'$, one concludes that the elastic energy (per unit length of dislocation) *decreases*

$$\Delta F_{\mathrm{el}} = -[K_1 b^2/(16\sqrt{2\pi d''}\lambda_1^{3/2})]\left(\sqrt{\frac{d''}{d'}} - 1\right). \quad (5)$$

On the other hand, the layers tilt $\theta_\infty \approx \partial u/\partial x \approx b \exp(-\frac{x^2}{4\lambda_1 d})/(4\sqrt{\pi\lambda_1 d})$ and the associated anchoring energy

$$\Delta F_{\mathrm{surf}} \approx \frac{1}{4} W_p \int_{-\infty}^{\infty} (\theta_\infty^2|_{d=d'} - \theta_\infty^2|_{d=d''})dx \approx [(W_p b^2)/(32\sqrt{2\pi\lambda_1 d''})]\left(\sqrt{\frac{d''}{d'}} - 1\right), \quad (6)$$

both *increase* when the dislocation is brought closer to the D plate. Here we assume $W_p\theta_\infty \ll 2\sqrt{K_3 B}$; i.e., $W_t(\theta_\infty) \approx \frac{1}{4} W_p \theta_\infty^2$ in Eq. (4). As is easy to see, $\Delta F_{\mathrm{el}} + \Delta F_{\mathrm{surf}} \propto (K_1/\lambda_1 - W_p/2)(1 - \sqrt{d''/d'}) = 0$ when $W_p = 2\sqrt{K_1 B}$; the dislocation-plate interaction vanishes. For $W_p < 2\sqrt{K_1 B}$, the dislocation is attracted to the plate, and for $W_p > 2\sqrt{K_1 B}$ it is repelled. The results for $W_t(\theta_\infty) \approx \frac{1}{4} W_p \theta_\infty^2$ are similar to those in the theory of surface-tension mediated interaction; in the latter case the critical value of surface tension is $\sqrt{K_1 B}$ [1,13]. For a more accurate description, especially when the condition $W_p\theta_\infty \ll 2\sqrt{K_3 B}$ is not valid, one should use the complete form of Eq. (4). Numerical analysis of Eq. (4) [14]

shows that the critical value $W_{p,\mathrm{crit}} = 2\sqrt{K_1 B}$ does not change much; however, further studies are needed to explore, for example, whether the dislocation can be in equilibrium at some finite distance from the plate in a semi-infinite sample when $W_p \sim 2\sqrt{K_1 B}$, $2\sqrt{K_3 B}$.

$W_{p,\mathrm{crit}}$ can be estimated by expressing K_1 and B through the Frank constants [4] of ZLI3412 for twist, $K_{22} = 6.7\,\mathrm{pN}$, and bend, $K_{33} = 15.5\,\mathrm{pN}$. One finds $K_1 = 3K_{33}/8 = 5.8\,\mathrm{pN}$, $B = K_{22}(\frac{2\pi}{p_0})^2 = 10.6\,\mathrm{J/m^3}$, and $W_{p,\mathrm{crit}} \sim 0.2 \times 10^{-4}\,\mathrm{J/m^2}$, close to the experimental W_p at WD plates. The data in Fig. 3 for the dislocation confined between two WD plates correspond closely to the case $F_{\mathrm{el}} + F_{\mathrm{surf}} \approx 0$, as the dislocation profile fits well the theoretical model for a dislocation in an infinite medium [11]. In contrast, $W_p = (4 \pm 1) \times 10^{-4}\,\mathrm{J/m^2}$ at SU plates is an order of magnitude larger than $2\sqrt{K_1 B}$ and thus the dislocation is expected to repell from them, as observed. A nonzero W_a at rubbed SU plates can enhance this repulsion. The glide of dislocation away from the SU and towards the WD plate in Fig. 2 can be caused by both repulsion from the SU plate and (weak) attraction to the WD plate. We stress again that the glide is hindered by Peierls-Nabarro friction associated with the peculiar split core of dislocations and occurs via kinks [2,7].

To conclude, we visualized the director patterns in vertical cross sections of cholesteric samples bounded by rigid plates and demonstrated that the behavior of edge dislocation strongly depends on the anchoring properties of the bounding plates. Edge dislocations can be expelled from the sample in which one of the plates has a weak polar anchoring and no azimuthal anchoring. The Burgers vector of dislocations in weakly anchored samples is always $b = p$ and never $b = p/2$. In SU-WD wedges, each dislocation separates two regions in which the cholesteric twist changes by π, in contrast to the classical strongly anchored Grandjean-Cano wedges in which the dislocations $b = p$ stay close to the bisector plane and separate regions with twist difference 2π [7]. We proposed a coarse-grained model of CLC anchoring for plates with no azimuthal anchoring and arbitrary polar anchoring which predicts that the dislocation-plate interaction vanishes when $W_p \approx 2\sqrt{K_1 B}$; repulsion is expected for larger W_p and attraction for smaller W_p.

The work was supported by NSF ALCOM Grant No. DMR89-20147-13 and by the Donors of the Petroleum Research Fund, Grant No. 35306-AC7. We thank I. Dozov, T. Ishikawa, E. I. Kats, M. Kleman, N. Madhusudana, Ph. Martinot-Lagarde, and S.V. Shiyanovskii for useful discussions.

*Corresponding author.
Electronic address: odl@lci.kent.edu

[1] R. Hołyst and P. Oswald, Int. J. Mod. Phys. B **9**, 1515 (1995).
[2] M. Kleman and O. D. Lavrentovich, *Soft Matter Physics: An Introduction* (Springer-Verlag, New York, 2003).
[3] M. Maaloum *et al.*, Phys. Rev. Lett. **68**, 1575 (1992); M. S. Turner *et al.*, J. Phys. II (France) **4**, 689 (1994).
[4] P. G. de Gennes and J. Prost, *The Physics of Liquid Crystals* (Clarendon Press, Oxford, 1993).
[5] I. I. Smalyukh, S.V. Shiyanovskii, and O. D. Lavrentovich, Chem. Phys. Lett. **336**, 88 (2001).
[6] S.V. Shiyanovskii, I. I. Smalyukh, and O. D. Lavrentovich, in *Defects in Liquid Crystals: Computer Simulations, Theory and Experiments*, edited by O. D. Lavrentovich, P. Pasini, G. Zannoni, and S. Zŭmer, NATO Science Series (Kluwer Academic Publishers, Dordrecht, 2001), Vol. 43, p. 229.
[7] I. I. Smalyukh and O. D. Lavrentovich, Phys. Rev. E **66**, 051703 (2002).
[8] Yu. A. Nastishin, R. D. Polak, S.V. Shiyanovskii, and O. D. Lavrentovich, Appl. Phys. Lett. **75**, 202 (1999).
[9] O. Ramdane *et al.*, Phys. Rev. Lett. **84**, 3871 (2000).
[10] D. N. Stoenescu *et al.*, Mol. Cryst. Liq. Cryst. **358**, 275 (2001).
[11] E. A. Brener and V. I. Marchenko, Phys. Rev. E **59**, R4752 (1999).
[12] T. Ishikawa and O. D. Lavrentovich, Phys. Rev. E **60**, R5037 (1999); T. Ishikawa and O. D. Lavrentovich, in *Defects in Liquid Crystals: Computer Simulations, Theory and Experiments* (Ref. [6]), Vol. 43, p. 271.
[13] L. Lejcek and P. Oswald, J. Phys. II (France) **1**, 931 (1991).
[14] K_3 can be derived from the Kats-Lebedev theory (E. I. Kats and V.V. Lebedev, *Fluctuational Effects in the Dynamics of Liquid Crystals* (Springer-Verlag, New York, 1994, p. 170); $K_3 = \frac{K_{11}K_{33}}{2(K_{11}+K_{33})}$, as first calculated by E. I. Kats.